Cement & Concrete Composites 34 (2012) 1202–1209

Contents lists available at SciVerse ScienceDirect

Cement & Concrete Composites

journal homepage: www.elsevier.com/locate/cemconcomp

Effects of reinforcement configuration and sustained load on the behaviour of reinforced concrete beams affected by reinforcing steel corrosion

L. Hariche [a], Y. Ballim [b], M. Bouhicha [c], S. Kenai [a,*]

[a] Civil Engineering Department, University of Blida, Algeria
[b] School of Civil & Environmental Engineering, University of the Witwatersrand, Johannesburg, South Africa
[c] Civil Engineering Department, University of Laghouat, Algeria

ARTICLE INFO

Article history:
Received 2 October 2010
Received in revised form 28 July 2012
Accepted 30 July 2012
Available online 4 August 2012

Keywords:
Concrete
Corrosion
Sustained load
Serviceability
Deflection
Cracking
Durability

ABSTRACT

Corrosion of reinforcing steel bars in concrete is one of the main causes of early deterioration and reduction of service life of reinforced concrete (RC) structures. This paper reports on the results of an experimental programme that was carried out to study the effect of reinforcement corrosion on the serviceability behaviour of RC beams under load. The main parameters investigated were the effects of reinforcement arrangement and the magnitude of the sustained load. Four series of scaled beams were tested, each series containing six beams, three of which were subjected to reinforcement corrosion while the other three were used as un-corroded control beams. All these beams carried the same sustained load during the process of reinforcement corrosion. The reinforcement arrangement for the fourth test series was identical to the first series but these beams carried a higher sustained test load. All the beams were subjected to a four-point bending load arrangement. Corrosion of the tension reinforcement was accelerated using an impressed current while the soffits of the beams were immersed in a 3% sodium chloride solution. The evolution of reinforcement corrosion and central deflection under simultaneous load and corrosion is given. The deflections of the beams increase with progressive corrosion of the reinforcement especially during the early stages of corrosion as a result of propagation of transverse cracks and the expansive stresses induced by the corrosion products. The importance of the arrangement of the steel in the section of concrete on the performance in terms of deflection was also clarified.

1. Introduction

The success of reinforced concrete (RC) is due mainly to its structural versatility, long-term durability characteristics and the complementary interaction of its materials, namely the reinforcing steel and concrete. Provided that appropriate measures were undertaken in the design and the construction of a reinforced concrete structure, reinforcing steel embedded in concrete is normally protected against corrosion during the service life of the structure. However, this concrete cover protection to the reinforcement can be deteriorated by aggressive agents leading to the corrosion of the steel in concrete.

Internationally, the corrosion of reinforcing steel bars is the principal cause of early deterioration of concrete structures, leading to a reduction in residual service life. When aggressive agents reach the reinforcement due to chloride attack or carbonation of concrete cover, corrosion may start affecting [1]:

- the steel, due to the reduction of both the bar section and the mechanical properties [2],
- the concrete, due to the cover cracking provoked by the expansion of corrosion products [3],
- the composite action of concrete and steel, due to the bond deterioration [4].

The combined effect of increased cracking and bond slippage results in increased serviceability deflection of the beams.

Most of the research works found in the literature that try to assess this phenomenon were based on laboratory studies. To reduce the time necessary for the corrosion of reinforcing bars, acceleration procedures such as impressing an electrical current on the steel or adding sodium chloride solution to the mixing water of concrete were used. Moreover, in the majority of the work reported in the literature, the corrosion of steel bars was carried out before load-testing of the RC elements. Ballim et al. [5,6] pointed out that this testing procedure presents two main drawbacks:

- In real structures, the corrosion takes place while the structure carries load and the two effects act synergistically to accelerate the deterioration of the structure. For example, in the case of a

* Corresponding author. Address: Geomaterilas Laboratory, Civil Engineering Department, University of Blida, PO Box 270, Bliuda, Algeria. Tel./fax: +213 25433639.
E-mail address: sdkenai@yahoo.com (S. Kenai).

0958-9465/$ - see front matter © 2012 Elsevier Ltd. All rights reserved.
http://dx.doi.org/10.1016/j.cemconcomp.2012.07.010

beam element, cracks induced by the corrosion products are widened by the effects of the applied loads (and vice versa), thus allowing greater access to oxygen and water for more rapid corrosion than if the load effects were not simultaneously imposed.

- During the corrosion process, the time-dependent effects of a sustained load on serviceability limit state behaviour are not considered. The level of corrosion related stresses and the duration and the level of external loads are both influencing factors in the deformation of the structure.

Through laboratory-based study, the research work reported in this paper assesses the structural performance of four series of scaled RC beams under simultaneous load and reinforcement corrosion conditions. The first three series of beams were subjected to the same test conditions except that the arrangement of the tensile reinforcement was varied.

This paper presents a brief description of the purpose-made loading rig and the method by which the reinforcement corrosion was accelerated. This is followed by a description of the experimental program, a presentation of the results and a discussion of their implications.

2. Description of the sustained loading test rig

The sustained load test rig developed by Ballim and Reid [5] was used in this testing programme (Fig. 1). Briefly, the loading rig allows a sustained four-point bending load to be applied to a simply supported reinforced concrete beam over a span of 1050 mm. The load is applied through a compressed spring, onto a spreader beam that is placed on the top of the test beam. For the samples subjected to accelerated corrosion of the tension reinforcement, the undersides of the test beams as well as the supports were located inside a plastic watertight tank containing an electrolyte (3% NaCl solution). A companion steel bar, which acts as the cathode for the accelerated corrosion process, was placed in the electrolyte solution below the beam. The same testing rig and arrangement was used for the control un-corroded samples, except that the electrolyte was replaced by plain water.

Six loading rigs were used to allow simultaneous testing of three beams with corroding reinforcement and three un-corroded control beams. One such set of six beams constituted a single test series.

Compression of the load spring was achieved by turning the nuts on threaded rods which passed through a movable plate.

Fig. 1. A general view of the loaded frames.

The magnitude of the load was controlled by monitoring the vertical compression of the spring. The springs were fabricated to provide a spring rate of 400 N/mm. By using a spirit level to ensure that the movable loading plate was horizontal during loading and a vernier depth gauge, it was possible to compress the spring to an accuracy of 0.1 mm. This translates to a load accuracy of approximately 0.04 kN.

The central deflections of the beams as well as the deflection of the beams over the support points were monitored using dial gauges attached to the main steel I-section. This allowed the central deflection of the beams to be determined relative to that of the supports. It should be noted that the supports points inside the electrolytic plastic tank were made from a hard plastic material.

3. Experimental program

3.1. Test beam dimensions and materials used

Twenty-four beams were cast with the dimensions and reinforcing layout shown in Fig. 2. The beams were divided equally into four series of six beams. In each series, the main tension reinforcing steel of three beams was subjected to accelerated corrosion while the three other un-corroded beams served as control. As stated before the two parameters investigated during this study were reinforcement arrangement and magnitude of loading. The first three series of beams were used to study the effect of tension steel arrangement, as shown in Fig. 2. The fourth series of beams were reinforced in an identical manner as the first series but was subjected to a higher applied load than in the case of the first three series of tests. The tensile reinforcement of the beams consisted of high tensile deformed bars (Y) whereas the shear links and compression (top) reinforcement was made of mild steel bars (R), cut and bent as appropriate. All the reinforcing steel was obtained from the same steel mill run and a sample of the Y12 bar was tested to give a 0.2% proof stress of 596 MPa.

The shear stirrups were covered with a section of heat-shrink plastic at the points of contact with the main tension steel bar. This was done to electrically isolate the rest of the steel cage from the main tensile bars that were to be corroded by an impressed current.

The concrete mixture used to make the beams and cube samples for compressive strength testing consisted of ordinary Portland cement (CEM1), crushed sand, water and 13.2 mm crushed gravel using the mixture proportions shown in Table 1. This concrete was designed according to guidance found in the literature [7] so as to yield target 28-day compression strength of 47 MPa. The crushed sand used had a fineness modulus of 2.86 and its grading satisfied the SABS 1083 [8] requirements. In the preparation of each series of six beams, sufficient concrete was mixed to also prepare three 100 mm cubes for compression strength testing and three 100 mm square $\times$ 200 mm high prisms for elastic modulus measurements in accordance to BS 1881 part 121 [9]. The concrete cube and prism samples were moist cured for 28 days at temperature of 22 ± 1 °C. The beams were wet cured until the age of test which varied between 30 and 130 days because of availability of testing rigs.

3.2. Instrumentation and loading of the test beams

An insulated electrical wire was soldered to one end of each tensile reinforcement bars before casting and the soldered area was coated with a thick layer of insulating paint. This wire was held in place when the concrete was cast so that it will be exited from the top face of the beam. A galvanostatic method was used

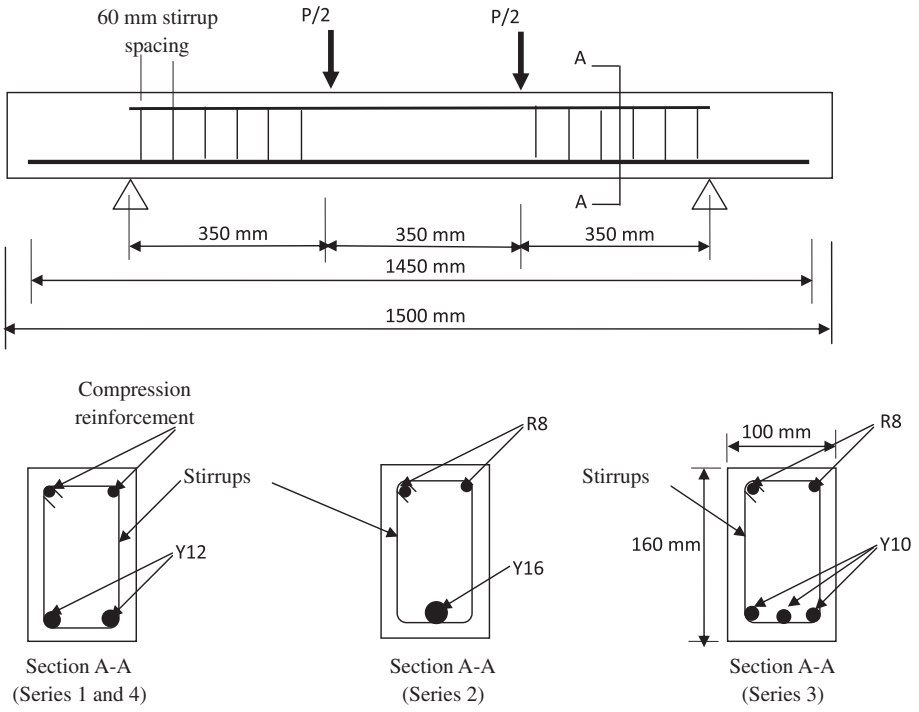

Fig. 2. Dimensions and reinforcement details of the concrete test beams.

Table 1
Mix proportion of the concrete used for preparing the beams.

Cement CEM I (kg/m^3)	409.1	
Gravel (kg/m^3)	1000	w/c = 0.55
Sand (kg/m^3)	849.6	Slump = 60 mm
Water (L/m^3)	225	

to accelerate the corrosion of the tensile reinforcement bars by connecting it to the positive terminal of a DC power supply, thus forcing the reinforcing steel to become anodic. The negative electrode was then connected to a steel rod (cathode) placed in the electrolytic solution.

The DC power supply, with a voltage limit of 30 V and a maximum current output of 3 A, was used to supply the corrosion current at a rate of approximately 150 mA/cm^2 of reinforcing steel surface. A data logger connected to a computer was used to record the current in the reinforcing bars every hour during the test period.

After curing, the beams were placed in the loading rig for testing. The soffit of the beams was immersed in the water or electrolyte solution to a depth of approximately 30 mm. As stated before, a 3% sodium chloride solution was used for the corroded beams whereas normal tap water was used for control beams. After a soaking period of one day in solution, the beams were loaded by compressing the springs to the required level and the resulting deflections were recorded as the elastic responses to the application of load. For the first three series of beams, the four-point load was set at 20 kN, whereas for the fourth series the four-point load was increased to 30 kN. The corrosion current was then applied to the reinforcing bars. Both the corrosion current and the applied loads were checked daily and adjusted to the set values if required. After the testing period, which generally exceeded 30 days under sustained load and simultaneous corrosion, the beams were removed from the loading rig and inspected visually for any corrosion damage that may have occurred. They were then placed in an Amsler testing machine with a load capacity of 2000 kN and tested to failure using the same 4 point bending loading arrangement.

Table 2
The degree of corrosion determined by gravimetric method (mass loss).

Test series	Beam no.	Tension bar number	Degree of corrosion (%)	Av. degree of corrosion (%)	Duration of accelerated corrosion period (days)
1	CR1	1	13.02	11.33	48
		2	9.65		
	CR2	1	11.73	11.69	
		2	11.65		
	CR3	1	11.51	12.37	
		2	13.22		
2	CR1	1	5.75	5.75	30
	CR2	1	5.96	5.96	
	CR3	1	5.94	5.94	
3	CR1	1	8.75	6.49	55 for Beam no 3 20 for Beams nos. 1 and 2
		2[a]	5.30		
		3	5.42		
	CR2	1	4.77	4.43	
		2[a]	3.40		
		3	5.13		
	CR3	1	15.20	19.43	
		2[a]	11.17		
		3	31.93		
4	CR1	1	7.98	9.18	32
		2	10.39		
	CR2	1	5.18	6.28	
		2	7.37		
	CR3	1	6.84	9.14	
		2	11.45		

[a] For the Series 3 beams, bar number 2 is the central bar.

3.3. Rate of corrosion calculation

Two methods were used to estimate the corrosion rate and are given as follows:

3.3.1. Gravimetric method

At the end of the test programme, the main tension reinforcement bars were carefully removed from each of the corroded beams and cleaned of all adhering mortar and corrosion product. The bars were then weighed to determine the extent of corrosion. The method used for cleaning the bars was similar to that outlined in ASTM G167 [10] and involved first brushing the bar with a brass bristle brush and brass wool and then dipping it into a dilute inhibited phosphoric acid solution.

3.3.2. Faraday's law

This method was used to determine a theoretical relationship between the time over which the impressed current was allowed to flow and the extent of corrosion [5,11,12]. The corrosion is an electrochemical reaction which means it results in a production of electrons. Assuming that, the oxidation of iron to ferrous ions ($Fe \rightarrow Fe^{2+} + 2e^{-}$) represents the principal electrochemical reaction, the charge that passes the circuit at time t after the start of the impressed current can be written using Faraday's law:

$$q_t = m \cdot n \cdot F = \frac{m_c}{w} \cdot n \cdot F \tag{1}$$

where q_t is the total charge (Coulombs) passed through the circuit after time t; m is the number of moles of reactant consumed (or product formed); n is the number of electrons required to convert reactant to product; F is Faradays constant (96 485 C/mol); m_c is the mass of the original iron consumed (g); w is the molar mass of the iron (=55.85 g/mol for Fe).

The charge can be determined by integrating the impressing current, I, with respect to time as follows:

$$q_1 = \int_{t=0}^{t} Idt \tag{2}$$

Combining Eqs. (1) and (2) yields the following equation, from which the mass of corrosion product can be determined at any time during the accelerated corrosion process:

$$m_c = \frac{q_t w}{nF} \tag{3}$$

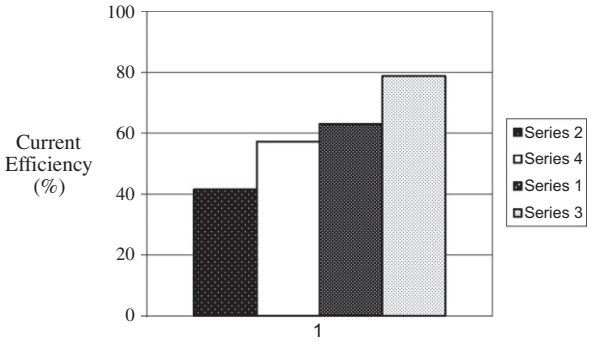

Fig. 3. Current efficiency.

Fig. 4. Appearance of the corroded steel.

q_t was calculated by numerically integrating the hourly measurements of impressed current over the time of testing, using the procedure described below.

The Trapezoidal formula was used to calculate the integral numerically, using the following approach:

$$q_0 = 0 \tag{4}$$

$$q_1 = q_0 + 3600\frac{I_0 + I_1}{2} \tag{5}$$

$$q_2 = q_1 + 3600\frac{I_1 + I_2}{2} \tag{6}$$

where q_1 and q_0 are in coulombs and I_1 and I_2 in Amperes, and more generally:

$$q_i = q_{i-1} + 3600\frac{I_{i-1} + I_i}{2} \tag{7}$$

Fig. 5. Maximum diameter (above the bar) and minimum diameter (below the bar) (in mm) of the corroded bars measured at various positions along the length of each bar after corrosion and cleaning.

The total charge q_t can thus be estimated every hour which in turn yields the hourly estimate of the lost mass of steel (m_c). If m_o is the original mass of the un-corroded bar, the percentage corrosion (C_t) with reference to the original mass, is given by:

$$C_t = \frac{(m_o - m_c)100}{m_o} \tag{8}$$

However, in reality, the $Fe \rightarrow Fe^{2+} + 2e^-$ is not the only reaction which takes place at the anode. There are competing reactions and

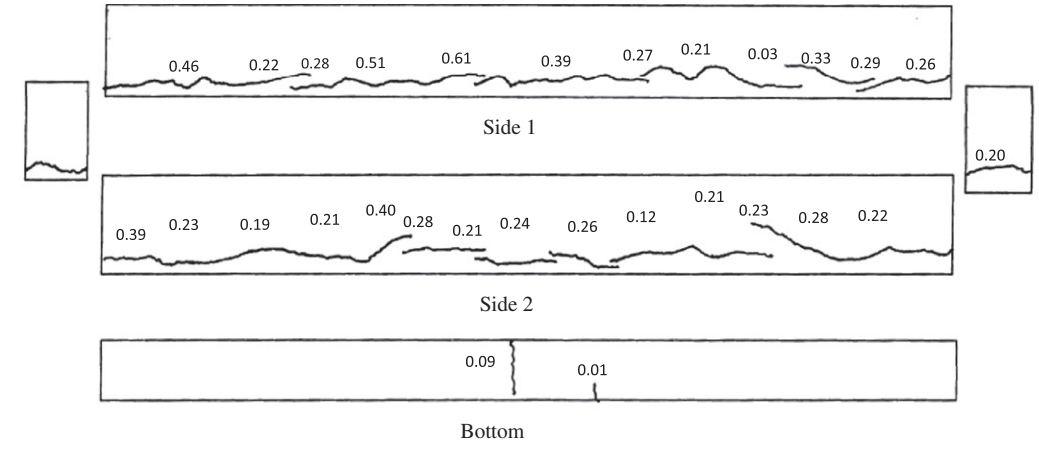

(a) Beam CR1 Series 1 (reinforcement bar 1 and 10)

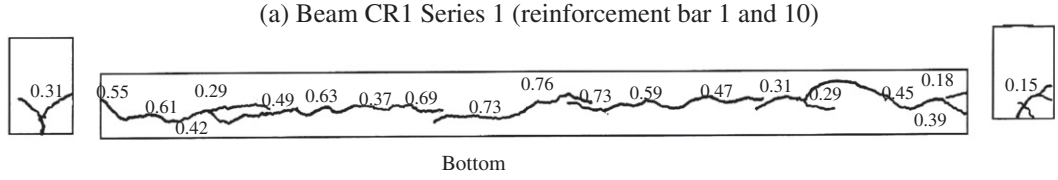

(b) Beam CR1 Series 2 (reinforcement bar No 3)

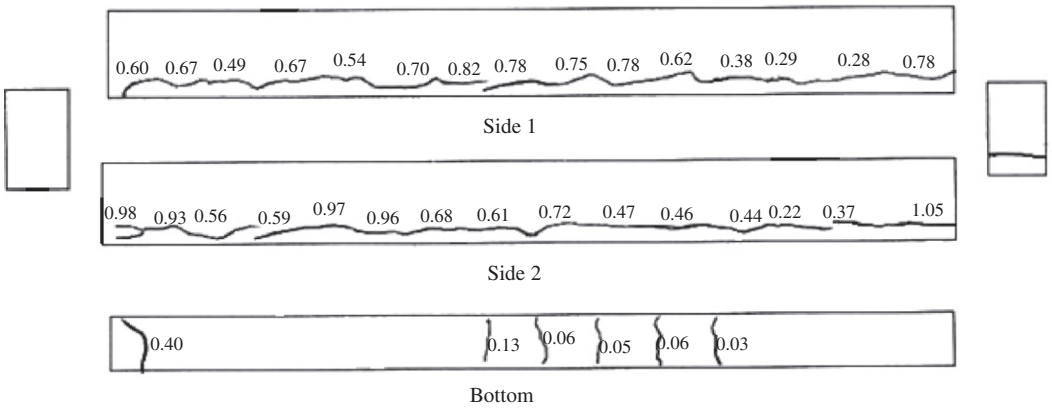

(c) Beam CR1 Series 3 (reinforcement bar No 1, 2 and 3)

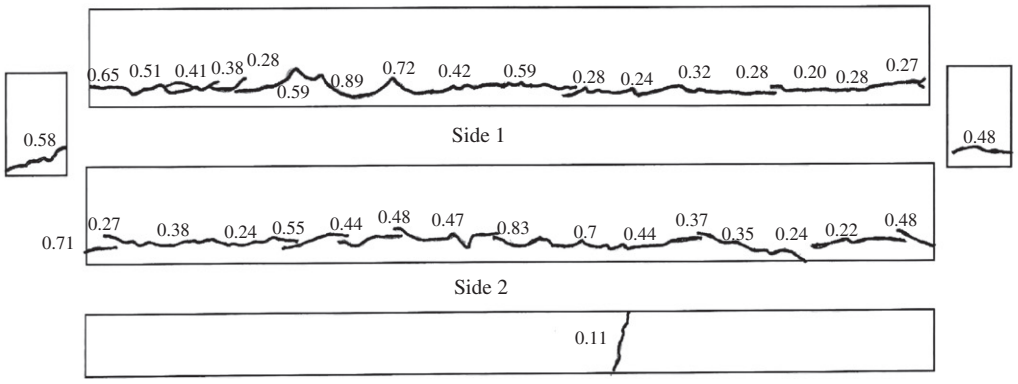

(d) Beam CR1 series 4 (reinforcement bar No 1 and 6)

Fig. 6. Cracking pattern and crack widths (in mm) for the four series of test beams.

Faraday's law will only give a true reflection of the extent of corrosion if all the electron equivalents which have entered in the reaction are used in the corrosion of the reinforcing steel. It is therefore necessary to determine the ratio of the charge consumed in the reaction of interest (oxidation of Fe in the reinforcing steel) to the total charge passed. This ratio is referred to as the current efficiency, N [13,14], and was obtained by comparing the mass of corrosion product determined from the gravimetric method to that given by Eq. (3) for the total accelerated corrosion period. This value of N was then used to adjust the extent of corrosion determined using Eq. (3) at various times during the corrosion process.

4. Results and discussion

4.1. Extent of corrosion

As mentioned above, two methods were used to estimate the rate of corrosion: gravimetric method and Faraday's law. The results obtained by the first method are summarised in Table 2. The values given by Faraday law were adjusted by multiplying them by current efficiency factor N. The values of N obtained for the series of beams tested are shown in Fig. 3. The results seem to indicate that the current efficiency increases when arrangement of small diameter reinforcing bars are used.

Upon removal from the concrete, all the corroded bars generally showed pitting corrosion with some areas of more concentrated corrosion, as shown in Fig. 4. This is in accordance to what was reported in the literature [14–16] and may be explained by the absence of carbonation of concrete, which would generally lead to more uniformly distributed corrosion.

The positions of the areas of concentrated corrosion can be identified in Fig. 5, which shows examples of the measured diameters of the reinforcement bars at different locations along their lengths. The values above and below the bars are the maximum and minimum diameters measured in that position along the length of the bar. It can be seen important scatters on the distribution of the steel cross-section losses along the same bar. The higher steel cross-section losses show clearly the areas of pitting corrosion along the bars. The pitting corrosion was observed to be focused at both the middle which corresponds to the zone where the bending moment is the most important and at the electrical connection end of the steel bars. This is most probably caused by electrical current concentration at the electrical connection end region and by higher steel stress together with increased concrete cracking in the middle section.

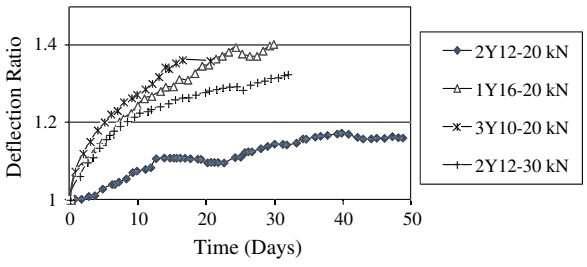

Fig. 7. Mid-span deflection ratios of control beams with time.

Table 3
Percentage of deflection variation of control beams.

Series	f_{c28} (MPa)	Age at the beginning of loading (days)	Loading duration (days)	% of deflection variation
Series 1	48.1	130	55	13
Series 2	45.9	30	30	30
Series 3	42.44	100	55	37
Series 4	43.79	34	32	24

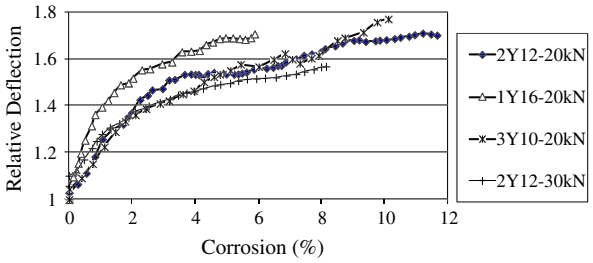

Fig. 8. Relative deflections of corroded beams with rate of corrosion.

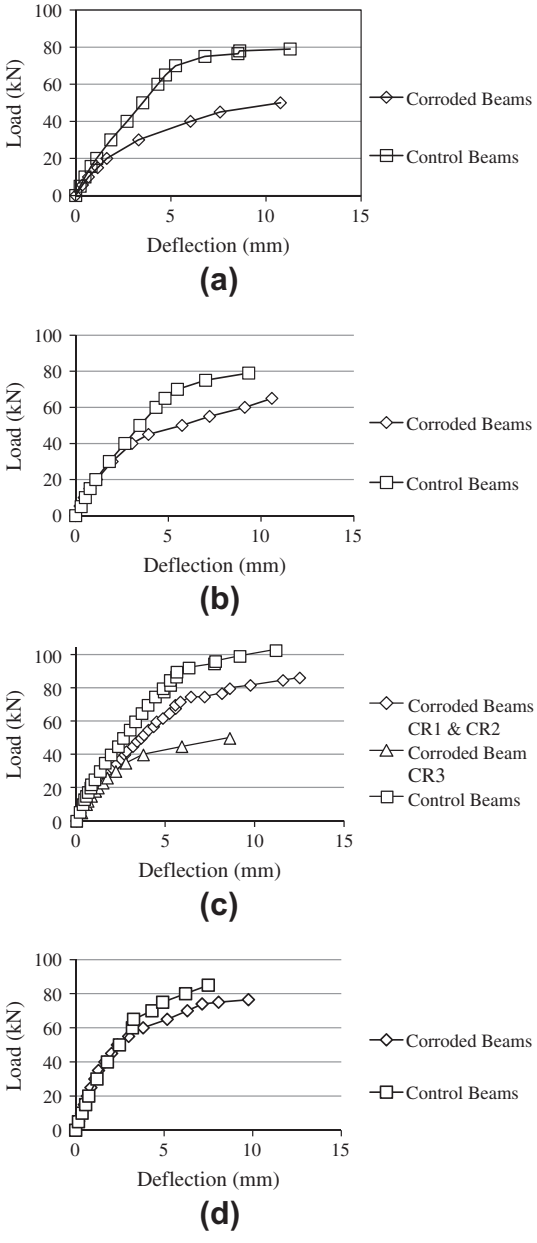

Fig. 9. Load–deflection curves for beams tested to failure. (a) Series 1, (b) Series 2, (c) Series 3, and (d) Series 4.

Table 4
Ultimate load results of corrosion beams.

Series	Beam no.	Rebar no.	Degree of corrosion (weight loss method) (%)	Average degree of corrosion (%)	Ultimate load of corroded beams (kN)	Average ultimate load of control beams (kN)	% Reduction in flexural strength
2Y12 20 kN	CR1	1	13.02	11.34	38	86.67	56.15
		10	9.65				
	CR2	3	11.73	11.69	54		37.69
		7	11.65				
	CR3	6	11.51	12.37	44		49.23
		9	13.22				
1Y16 20 kN	CR1	3	5.75	5.75	70	83.27	15.94
	CR2	2	5.96	5.96	71.6		14.01
	CR3	1	5.94	5.94	69		17.14
3Y10 20 kN	CR1	1	8.75	6.49	93.6	104.27	10.23
		2	5.30				
		3	5.42				
	CR2	4	4.77	4.43	94.4		9.47
		5	3.40				
		6	5.13				
	CR3	7	15.20	19.43	50.4		51.66
		8	11.17				
		9	31.93				
2Y12 30 kN	CR1	6	7.98	9.19	78.2	91.6	14.63
		1	10.39				
	CR2	2	5.18	6.28	80.2		12.45
		3	7.37				
	CR3	4	6.84	9.15	79.8		12.88

4.2. Cracking patterns

The beams were cleaned after corrosion testing and the cracking patterns as well as crack widths were measured and recorded. Typical crack patterns and crack widths are shown in Fig. 6a–d for the four series of tests.

It can be seen that longitudinal cracking occurred mainly on the sides of the beams for Series 1 (2Y12) and Series 3 (3 × Y10) while for series 2 (1 × Y16) a soffit longitudinal crack was observed. The choice of steel arrangement therefore appears to have a strong influence on the nature and extent of damage to concrete cover when the steel corrodes.

4.3. Deflection behaviour at serviceability limits state

4.3.1. Deflection of control beams

Fig. 7 shows the mid-span deflections ratios of control beams where the increase in deflection is mainly due to time dependent effect such as creep. Table 3 gives the relative increase in deflection at mid span, the duration as well as the age of loading and the compression strength of concrete used to make these control beams. It can be noticed that the creep effect decreases when either the strength of concrete increases [7,17,18] or the age of concrete at loading increases.

4.3.2. Deflection of corroded beams

The relative deflection of the corroded beams was obtained by dividing their deflections by the corresponding deflections of the control beams at the same time under load. The variation of the relative deflection with the rate of corrosion is shown in Fig. 8 for the series of beams considered herein. Relative deflection seems first to increase linearly with the rate of corrosion, then this increase is reduced once the rate of corrosion surpasses 2–4%. Moreover, the curves of series one, three and four are very similar whereas relative deflection for the Series 2 beams is the highest for all rates of corrosion considered. Consequently, the arrangement of soffit reinforcement seems to have a great influence not only on the cracking pattern but also on the increase of the corrosion caused deflection.

4.4. Deflection behaviour at ultimate state

As indicated earlier, once the corrosion testing was ended, the beams were placed in an Amsler testing machine and loaded to failure. The load deflection curves obtained during the ultimate loading tests for all the series of beams are shown in Fig. 9. Table 4, on the other hand, summarises the results obtained from these tests.

In the initial stage of loading, the load–deflection curves of the corroded and the control beams are identical indicating, thus, that the corroded beams recovered their stiffness when unloaded. However, as a result of damage caused by corrosion, the post cracking stiffness of the corroded beams is markedly lower than that of the control beams. Moreover, the drop in the flexural capacity of the beams can be clearly seen from the results reported in Table 4. This drop seems to depend on the extent of corrosion of the steel bars and the ratio of applied load to the ultimate load. To emphasise this, the variation of the relative failure load, which is defined

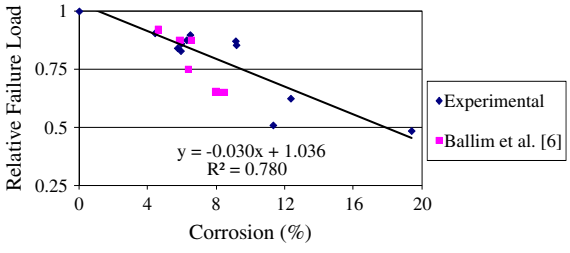

Fig. 10. Relative failure load vs. rate of corrosion.

as the ratio of the collapse load of the corroded beam to that of the control beam, with the corrosion extent is shown in Fig. 10. The drop in the flexural capacity becomes more substantial when the rate of corrosion is increased, and a linear relationship between the two parameters may be considered for design purposes [19].

5. Conclusion

The following conclusions can be drawn from this experimental and analytical investigation:

- In the process of acceleration of corrosion, the current efficiency is higher for a single large bar ($1 \times$ Y16) than for smaller bars ($2 \times$ Y12 or $3 \times$ Y10). This means that, to accelerate the corrosion of small diameter reinforcing steel bars, more current is needed than with bigger diameter bars, for the same level of corrosion. A further implication is that, when an RC structure is exposed to stray currents, there is likely to be a lower rate of corrosion if the structure is reinforced with smaller diameter bars, rather than in large ones.
- Because corrosion was initiated by the ingress of chloride ions into the concrete, the reinforcing steel in this series of tests showed predominantly pitting corrosion.
- Under simultaneous load and accelerated corrosion, the deflections of the beams increase with progressive corrosion of the reinforcement. A large increase in deflection was noted during the early stages of corrosion as a result of propagation of cracks on the tension side of the beams, caused by the flexural tension and the expansive stresses induced by the corrosion products. In addition, an increase of the ratio of applied load to the ultimate load increases the drop in the flexural capacity.
- This investigation has highlighted the importance of the form and distribution of reinforcing steel on the tension side of RC beams when deterioration due to corrosion is a concern. In spite of steel sectional area being nearly the same, the beams with two Y12 bars and those with three Y10 bars performed better in terms of deflection than the beams containing only a single Y16 bar as tension reinforcement.

References

[1] Rodriguez J, Ortiga LM, Casal J. Load carrying capacity of concrete structures with corrosion reinforcement. Constr Build Mater 1997;11(4):239–48.
[2] Andrade C, Alonso C, Garcia D, Rodriguez J. Remaining life time of reinforced concrete structure; Effet of corrosion on the mechanical properties of steel. In: International conference on life prediction of corrodible structures, Cambridge, UK; 1991. p. 12/1–11.
[3] Andrade C, Alonso C, Molina FJ. Cover cracking as a function of bar corrosion Part 1: experimental test. Mater Struct 1993;26:453–64.
[4] Rodriguez J, Ortega LM, Castel J. Corrosion of reinforcing bars and service life of reinforcing concrete structure: Corrosion and bon deterioration. In: International conference on concrete across borders, Odense, Denmark, vol. 2; 1994. p. 315–26.
[5] Ballim Y, Reid JC. Reinforcement corrosion and the deflection of RC beam-an experimental critique of current test methods. Cem Concr Compos 2003;25:625–32.
[6] Ballim Y, Reid JC, Kemp AR. Deflection of RC beams under simultaneous load and steel corrosion. Mag Concr Res 2001;53(3):171–81.
[7] Addis B, Owens G, editors. Fulton's concrete technology. Midrand (South Africa): Cement & Concrete Institute; 2001.
[8] SABS 1083. Specification for aggregates from natural sources. South Africa Bureau of standards, Pretoria, South Africa; 1976.
[9] BS 1881: 1983. Testing concrete, Part 121 method for determination of static modulus of elasticity in compression. London: British Standards Institution; 1983.
[10] ASTM G1-67. Recommended practice for preparing, cleaning and evaluating corrosion test specimens. American Society for Testing and Materials, Philadelphia, PA; 1971.
[11] Cabrera JG, Ghoddousi P. The effect of reinforcement corrosion on the strength of the steel/concrete bond. In: Proceedings of the conference on bond in concrete, Latvia, CEB; 1992. p. 11–24 [Chapter 10].
[12] Broomfield JP. Assessing corrosion damage on reinforced concrete structures. In: Swamy RN, editor. Corrosion and corrosion protection of steel in concrete. Sheffield: Sheffield Academic Press; 1994. p. 1–25.
[13] Macinnes DA. The principles of electrochemistry. New York: Reynolds Publishing Corporation; 1939. p. 38–9.
[14] Raharinaivo A, Arliguie G, Chaussadent T, Grimaldi G, Pollet V, Taché G, et al. Corrosion et la protection des aciers dans le béton. Paris: Presses de l'école nationale des Ponts et Chaussées; 1998.
[15] Landolt D. Introduction to surface reactions: electrochemical basis of corrosion. In: Marcus P, editor. Corrosion mechanisms in theory and practice. New York: Marcel Dekker Inc; 2002. p. 1–18.
[16] Bardal E. Corrosion and protection. London: Springer Verlag; 2004.
[17] Macginley TJ, Choo BS. Reinforced concrete: design theory and examples. 2nd ed. London & New York: Spon Press Taylor & Francis group; 2003.
[18] Ghali A, Favre R, Elbadry M. Concrete structures: stresses and deformation. 3rd ed. London & New York: Spon Press; 2002.
[19] Cabrera JG. Deterioration of concrete due to reinforcement steel corrosion. Cem Concr Compos 1996;18:47–59.